Int. J. Electrochem. Sci., 5 **(2010)** 1898 - 1910

International Journal of
ELECTROCHEMICAL
SCIENCE
www.electrochemsci.org

Electrodeposition of Fe Powder from Citrate Containing Electrolytes

Lj. J. Pavlović[1,*], *M. M. Pavlović*[2], *M. G. Pavlović*[1], *N. D. Nikolić*[1], *M.V. Tomić*[3]

[1] University of Belgrade, Institute of Electrochemistry ICTM, 11000 Belgrade, Njegoševa 12, Serbia
[2] École Polytechnique Fédérale de Lausanne, LTC, 1015 Lausanne, Switzerland
[3] University of Eastern Sarajevo, Faculty of Technology, Zvornik, Republic of Srpska
[*]E-mail: buba@tmf.bg.ac.rs

Received: 4 November 2010 / *Accepted:* 15 November 2010 / *Published:* 1 December 2010

Polarization characteristics of the electrodeposition processes of Fe powders from different citrate electrolytes and the morphology of the obtained powders were investigated. The effect of complexing agents on the cathodic polarization, the current efficiency and morphology of electrodeposited Fe powders were investigated. The morphology of obtained powders depends on the kind of supporting electrolyte, but not on the current density in investigated range. A characteristic feature of powders deposited from citrate-chloride supporting electrolyte is cauliflower-like compressed structure. On the other side, Fe powders electrodeposited from citrate-sulfate supporting electrolyte appeared in the form of spongy-like agglomerates. Possibility of Fe powders protection from corrosion in the process of production and during long-term storing has been shown.

Keywords: Fe powder, morphology, polarization diagrams

1. INTRODUCTION

By the electrochemical classification of metals, the transition metals such as Fe, Ni and Co belong to the "inert metal" group, with small exchange current density j_0 and high overpotential of electrodeposition η [1,2]. A characteristic of all polarization diagrams recorded during the electrochemical deposition of metals and alloys powders of the Fe group is distinguished through the following phenomena: a) the deposition of powders (as well as compact metal) is accompanied by the simultaneous evolution of hydrogen from the very beginning of metal deposition. In this situation the plateau corresponding to the limited current density cannot be registered on the polarization diagram as is the case with copper [3]; b) all of the polarization diagrams corrected for the *IR* drop are characterized by the presence of two inflexion points, i.e. the first inflection corresponds to the

beginning of metal deposition which is then followed by the rapid rise of current density, whereas the second inflection characterizes the start of a linear change of current density with potential. This deviation from linearity demonstrates a change of metal deposition mechanism [4,5].

The physical and chemical characteristics of Fe determine its peculiar electrochemical behavior. Almost all data concerning electrodeposition of Fe powders are summarized by Calusaru [6]. A literature survey of Fe powders electrodeposition shows that mainly two types of electrolytes were investigated and these were based on sulfate [6-11] and chloride electrolytes [6,12]. In all reported cases the morphology of deposited powders was dendritic [8,13].

Fe powders have very high tendency of corrosion. The wet electrolytical product contains over 99% Fe, while the washed and dried powders may contain several percentage of oxide [8]. Kuzmin and Kiseleva [8] have shown the marked influence of pH values on the content of oxide in Fe powders electrodeposited from sulfate electrolytes. They investigated Fe (II) based electrolytes within pH ranges of 1.5-4.2. The oxide content depends not only on the amount of hydroxides formed during deposition, but also on the amount of powder oxidized during washing and drying. It is noteworthy that the lower the pH, the much lower is the oxide content.

This study presents the results of researches of the polarization characteristics of the processes of the electrodeposition of Fe powders from citrate-chloride and citrate-sulfate containing electrolytes, which have significantly higher pH value than until now investigated electrolytes and therefore lower possibility to dissolve Fe powder particles than in sulfate and chloride electrolytes.

The morphology of these powders and EDS analysis have also been investigated.

2. EXPERIMENTAL

The polarization diagrams were recorded in a three-compartment standard electrochemical cell at the room temperature. The platinum foil counter electrode and the reference-saturated silver/silver chloride (Ag/AgCl) electrode (E_{ref} =0.20V vs. NHE) were placed in separated compartments. The latter was connected to the working electrode by a Luggin capillary positioned at the distance of 0.2 cm from working electrode surface. The working electrode was glassy carbon rod (d=0.3 cm) sealed in epoxy resin so that only the surface area of the disc of 0.071cm^2 was exposed to the solution and was placed paralled to the counter electrode in a vertical position [14].

The polarization measurements were performed by computer-controlled potentiostat (PAR M273A) using the corrosion software (PAR M352/252, Version 2.01) with the sweep rate of 1mVs^{-1}. For obtaining polarization curves corrected for *IR* drop, current interrupt technique was used with time of current interruption being 0.5 s.

All powder samples were electrodeposited at the room temperature in the cylindrical glass cell of the total volume of 2 dm^3 with cone shaped bottom of the cell in order to collect powder particles in it. Working electrode was a glassy carbon rod with the total surface area of 1.0 cm^2 immersed in the solution and placed in the middle of the cell [14-17].

All solutions were prepared from analytical grade chemicals and distillated water by following procedure: $Na_3C_6H_5O_7$ was first dissolved; in the next step metal Fe(II) salts were dissolved, and

finally supporting electrolyte was added. The procedure must be followed in order to prevent oxidation of Fe^{2+} into Fe^{3+} ion [18,19].

Pure metal powders were electrodeposited from solutions containing: 0.1M $FeCl_2x4H_2O$ + 0.2M $Na_3C_6H_5O_7$ + 2.0M NH_4Cl as well as solution containing: 0.1M $FeSO_4x7H_20$ + 0.2M $Na_3C_6H_5O_7$ + 1M $(HN_4)_2SO_4$. pH of the investigeted solutions was 5.31 for citrate-chloride based solutions and 5.87 for citrate-sulfate based solutions respectively. Time of deposition was 5 min.

The wet powder was washed several times with a large amount of demineralized water until the wet powder was free from traces of acid. The powder was under water at all times to prevent oxidation. To inhibit oxidation in air, sodium soap SAP G-30 was added as additive to the water used for washing the Fe powder. Sodium soap SAP G-30 contains 78% of total fatty acids. The powder was then dried in the a furnace under a controlled nitrogen atmosphere at 110ºC [14,20].

The morphology of the electrodeposited powders was examined using scanning electron microscope (SEM), Tescan VEGA TS 5130MM equipped with an energy-dispersive X-ray spectroscopy (EDS), INCAP enta FET – X3, Oxford Instruments. Accordingly, composition of powders was determined by the EDS analysis.

3. RESULTS AND DISCUSSION

Experiments were performed from citrate electrolytes with addition of two supporting electrolytes: 2.0M NH_4Cl and 0.1M $(NH_4)_2SO_4$. NH_4Cl is supporting electrolyte for dissolving $FeCl_2$ x $4H_2O$ in $Na_3C_6H_5O_7$ solution, and $(NH_4)_2SO_4$ is supporting electrolyte for dissolving Fe_2SO_4 x $7H_2O$ in $Na_3C_6H_5O_7$ solution [18,19]. The supporting electrolyte did not influence the shape of the polarization curves and powder morphology in the presence of Fe (II) salts. The only difference was higher current density for powders electrodeposited from the electrolyte containing 2.0M NH_4Cl, and very small change in the position of polarization curves depending on the supporting electrolyte used. Conditions for Fe powder deposition are shown in Table 1.

Table 1. Fe powder electrodeposition conditions

Electrolyte	Deposition time [min]	Working electrode	Current density [Acm^{-2}]	Dimensions of working electrode
0.1M $FeCl_2$ x $4H_2O$ 0.2M $Na_3C_6H_5O_7$ 2.0M NH_4Cl pH=5.31	5	Glassy carbon	0.6 0.8 1.0	h = 1.0 cm d = 0.3 cm S = 1.0 cm^2
0.1M Fe_2SO_4 x $7H_2O$ 0.2M $Na_3C_6H_5O_7$ 1.0M $(NH_4)_2SO_4$ pH=5.87	5	Glassy carbon	0.4 0.5 0.6	h = 1.0 cm d = 0.3 cm S = 1.0 cm^2

It is well-known that the deposition of powders (as well as compact metal) of the Fe group is accompanied by simultaneous evolution of hydrogen from the very beginning of metal deposition [1-6]. This is the reason why the polarization curves in Figs. 1 (a and b) and 2 (a and b) are shown in following manner.

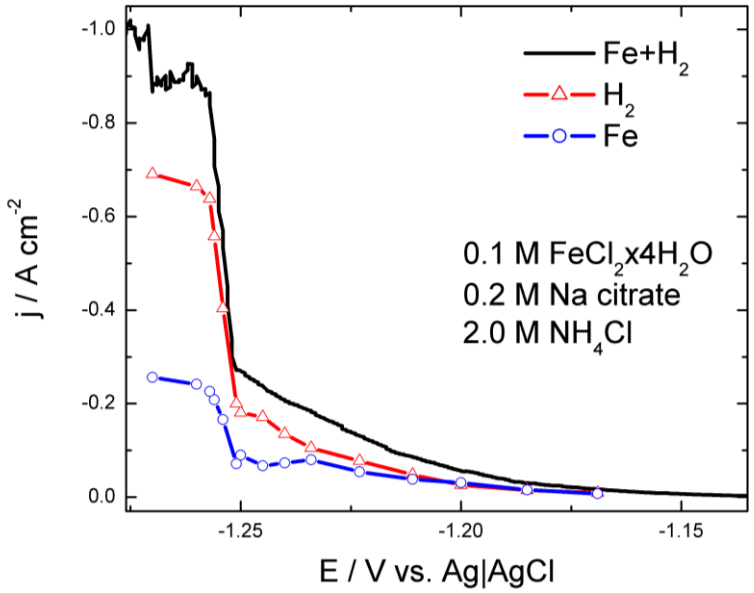

Figure 1(a). Polarization curves for the electrodeposition of Fe powder from the ammonium-chloride supporting electrolyte (0.1M $FeCl_2x4H_2O$ + 0.2M $Na_3C_6H_5O_7$ + 2.0M NH_4Cl) measured with IR drop correction

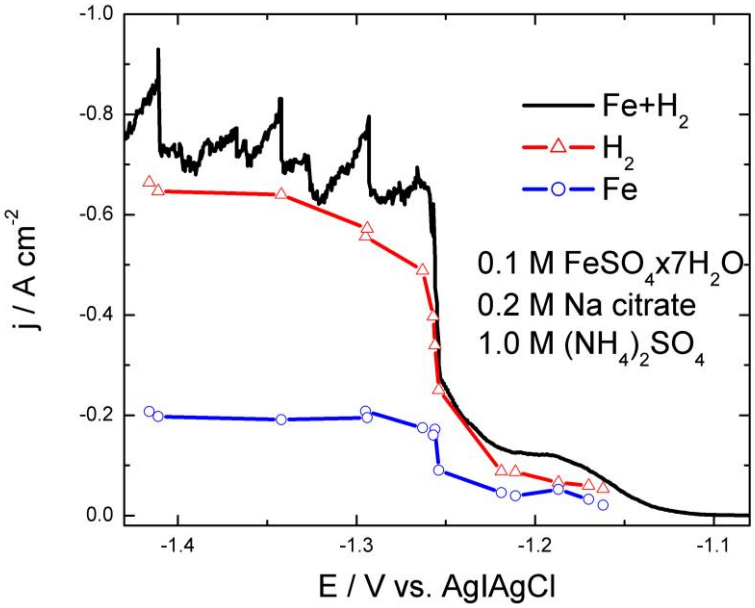

Figure 1(b). Polarization curves for the electrodeposition of Fe powder from the ammonium-sulfate supporting electrolyte (0.1M Fe_2SO_4 x $7H_2O$ + 0.2M $Na_3C_6H_5O_7$ + 1.0M $(NH_4)_2SO_4$) measured with IR drop correction

The polarization curves recorded in different electrolytes for Fe(II) salts are shown in Fig.1a (for ammonium-chloride supporting electrolyte) and Fig. 1b (for ammonium-sulfate supporting electrolyte), with correction for IR drop (Fe + H_2), polarization curve for hydrogen evolution (H_2) and polarization curve for Fe powder, after subtraction of j_{H_2}(Fe). Polarization curves for Fe powder electrodeposition and the corresponding η_j *vs. E* curves are illustrated in Figs. 2a and 2b.

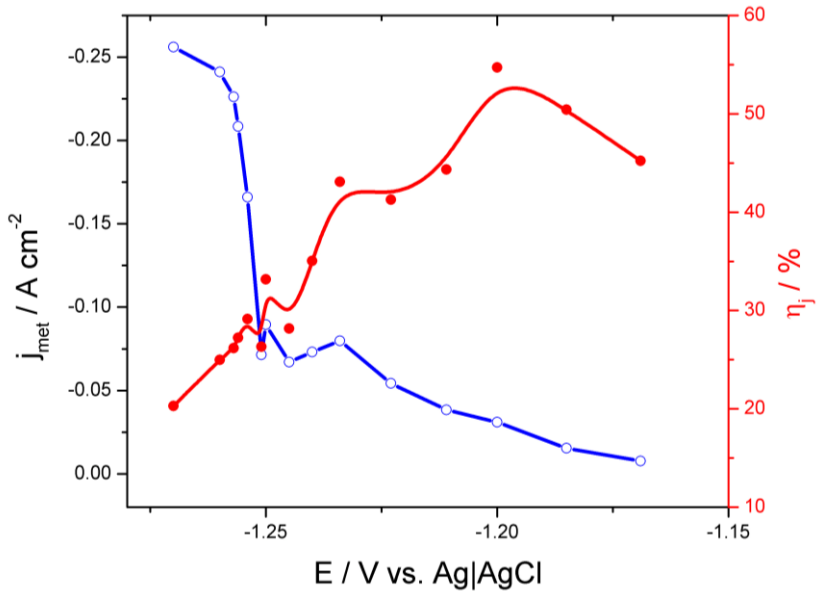

Figure 2(a). Polarization curve for Fe powder electrodeposition from the solution containing 0.1M $FeCl_2x4H_2O$ + 0.2M $Na_3C_6H_5O_7$ + 2.0M NH_4Cl and corresponding η_j(Fe) *vs. E* curve

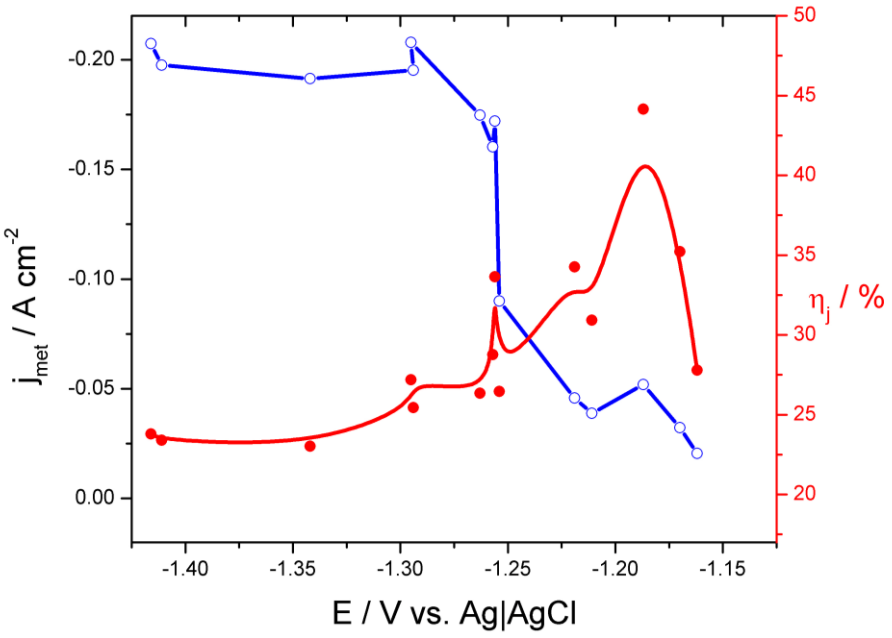

Figure 2(b). Polarization curve for Fe powder electrodeposition from the solution containing 0.1M Fe_2SO_4 x $7H_2O$ + 0.2M $Na_3C_6H_5O_7$ + 1.0M $(NH_4)_2SO_4$ and corresponding η_j(Fe) *vs. E* curve

From Fig. 1a and Fig. 1b it can be seen that the potential values at which the current density increases and at which the powder deposition starts are the same for both solutions and equal to -1.25V. Characteristics of all polarization diagrams for Fe powders electrodeposition is almost identical difference between diagrams with and without IR drop correction. As can be seen, in Figs. 1a and 1b, after IR drop correction, significantly different current response is obtained than the one measured without IR drop correction, being characterized by a sudden increase of current density at the commencement of the electrodeposition process. It is also characteristic that the processes of Fe electrodeposition were accompanied by hydrogen evolution in the whole range of the investigated potentials. As a consequence, extremely high currents were recorded and accordingly correction for IR drop caused significant change in the shape of the polarization diagrams. Another characteristic of all diagrams is that after sudden increase of current (in this case at about -1.25 V) an inflection point appeared on the polarization curves with further change of current showing linear increase with the potential.

Concerning the shape of the polarization curve for hydrogen evolution it could be concluded that such shape is a consequence of so called "electrode effect" [4, 21-26]. This phenomenon is connected with the bubble formation at high current densities, so that the evolution of the bubbles becomes the rate-limiting step of the electrochemical process [25,26], as explained in previous paper [5]. In accordance, the shape of the polarization curves for metals electrodeposition is also defined by the process of bubble evolution since the current for hydrogen evolution at more negative potentials (higher currents for metals or powders electrodeposition) in all cases amounts to 60% of the total current [27-33].

In Figs. 2a and 2b are shown polarization diagrams corrected for IR drop for the processes of Fe powders electrodeposition and corresponding η_j (Fe) *vs.* E curves. Limiting current density in the case of Fe powder deposition from sulfate supporting electrolyte than in chloride supporting electrolyte is higher for 0.05Acm^{-2}. Taking into account that simultaneous hydrogen evolution occurs during the process of powders electrodeposition, hydrogen evolution current density was determined from the volume of the evolved hydrogen at chosen current densities and subtracted from the total current density of electrodeposition. As seen in Fig. 2a and 2b correct polarization curves for Fe powders electrodeposition j_{met}, obtained by this procedure are much smaller than the total ones. Corresponding current efficiencies η_j obtained are also shown in these Figures. As can be seen η_j (Fe) start from high values of about 40-50%, sharply drop to about 20-25% and maintain this value in the region of the diffusion limiting current densities. At the same time current efficiency for metal electrodeposition (powder formation) obtained from chloride containing electrolyte is significantly higher than those in sulfate containing electrolyte.

In Figs. 3 and 4 are shown SEMs for Fe powders electrodeposited onto glassy carbon from citrate-chloride supporting electrolyte and citrate-sulfate one, respectively. In the case of electrodeposition onto glassy carbon electrode, two types of Fe powder particles are detected: cauliflower-like particles (chloride supporting electrolyte) of the size of about 150-200 μm and in sulfate supporting electrolyte (in the range of lower acidity) the deposits become spongy and sticky (some kind of fragile film - in the form of agglomerates).

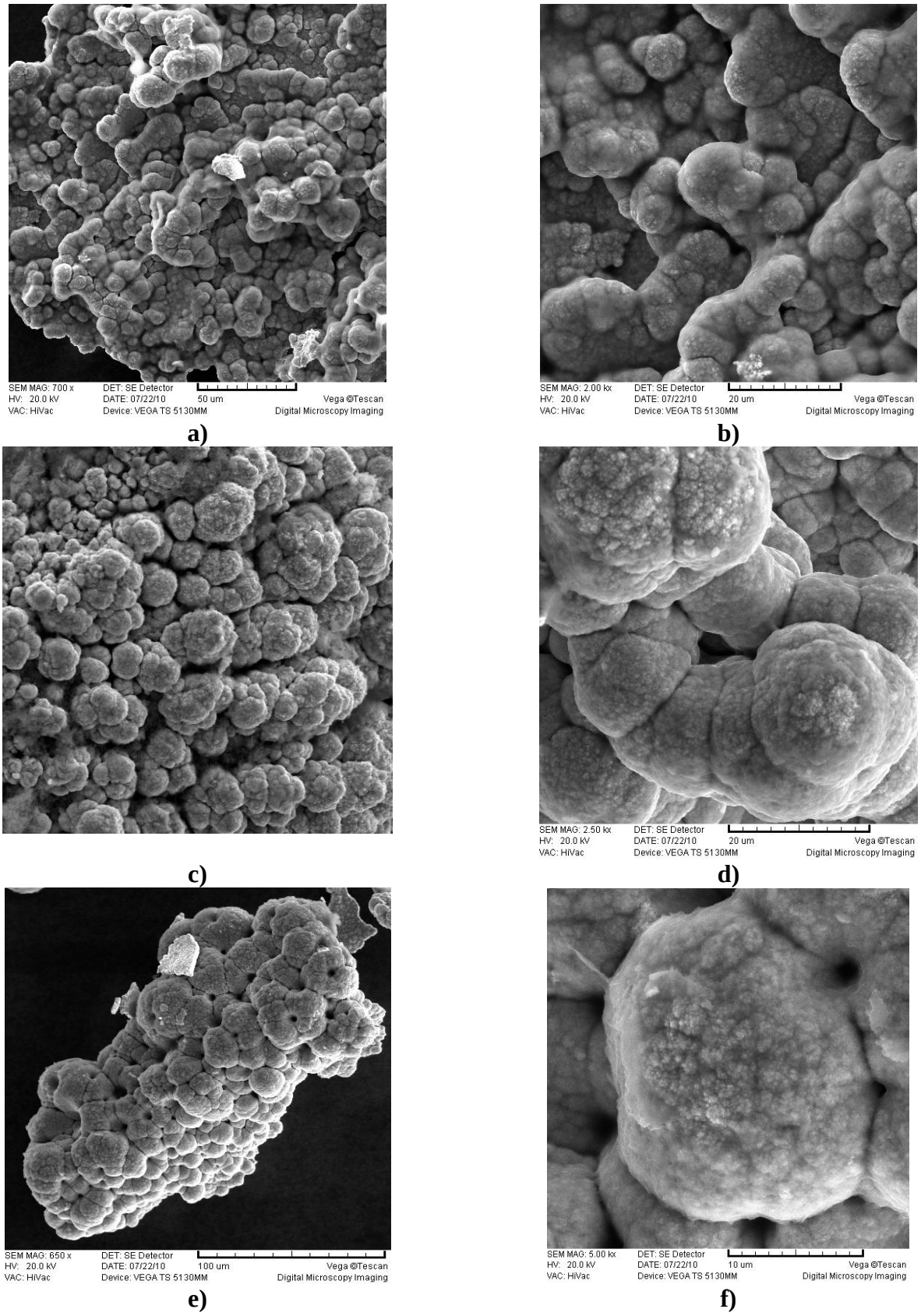

Figure 3. SEM micrographs of Fe powder electrodeposited onto glassy carbon electrode from the solution containing 0.1M $FeCl_2x4H_2O$ + 0.2M $Na_3C_6H_5O_7$ + 2.0M NH_4Cl. Morphology of the powder particles (a, c, e); morphology of the surface (b, d, f). j = 0.6 Acm^{-2} (a, b); j = 0.8 Acm^{-2} (c,d) and j = 1.0 Acm^{-2} (e,f).

It is likely possibly that the pH value of the electrolyte, which is higher than 5.31, as well as the influence of the sulfate lead to this kind of morphology of Fe deposit. It is characteristic for cauliflower-type particles that they completely fall off from the flat glassy carbon surface. Taking into account that at the beginning of the deposition process, before powder formation takes over the control of this process, a compact deposit must be formed at the substrate surface, it seems that partially a compact deposit is included in the powder particle. Cauliflower-like forms were obtained by electrodeposition at all applied current densities (chloride supporting electrolyte). Some of them were developed in dendritic forms or degenerated dendrites, a channel structure around dendritic and cauliflower-like particles. Generally, a cauliflower-type electrodeposit is produced when a spherical diffusion zone forms around the whole protrusion growing inside the diffusion layer of the macroelectrode [34]. By further increasing current density, hydrogen evolution becomes dominant process which leads to formation of great number of conical vacancies on the powder surface (Fig. 3e).

The main characteristics of open and porous structures formed in electrodeposition processes is that these structures are holes or pores formed by attached hydrogen bubbles which can be surrounded not only by agglomerates of metal grains but also by dendritic particles (Fig. 3a-f). Due to very high surface area of these structures, they are very suitable to be used as electrodes in many electrochemical devices, such as fuel cells, batteries and chemical sensors [35–37], as well as in catalysis [38].

Formation of so called “the honeycomb-like structures” can be briefly considered as follows: in the initial stage of the electrodeposition process, both nuclei of deposited metal and “nuclei” of hydrogen bubbles are formed at the active sites of the electrode surface [39].

The hydrogen bubbles isolate the substrate and then the current lines are concentrated around them making rings consisted of agglomerates of grains of deposited metal. The current lines are also concentrated at the metal nuclei formed in the initial stage between the hydrogen bubbles, thus forming metal grains agglomerates out of them. In the growth process, due to current density distribution effect, both hydrogen evolution and metal nucleation primarily occur at top of these agglomerates. Some of new, freshly formed hydrogen bubbles will coalesce with hydrogen bubbles formed in the initial stage of electrodeposition process, leading to their growth with electrolysis time. When the critical size for detachment from electrode surface of these hydrogen bubbles is reached, they will detach from electrode surface forming holes of regular shapes at electrode surface. Simultaneously, holes of irregular shapes are formed at electrode surface of agglomerates of metal grains formed between hydrogen bubbles. These holes are situated between regular holes. For longer electrodeposition time, coalescence of closely formed hydrogen bubbles occurs, leading to the formation of large, so-called “coalesced holes” [39]. This process makes the wall of the hole very porous. Meanwhile, some of new freshly formed hydrogen bubbles will not coalesce with previously formed hydrogen bubbles because they are situated between freshly formed iron nucleus, and these hydrogen bubbles have not enough place to develop in large hydrogen bubbles. These hydrogen bubbles will detach very fast from electrode surface forming channel structure through the interior of the deposit [30].

A spongy type of Fe powder particles (Figs. 4a, c, e) is characterized by the presence of deep cavities.

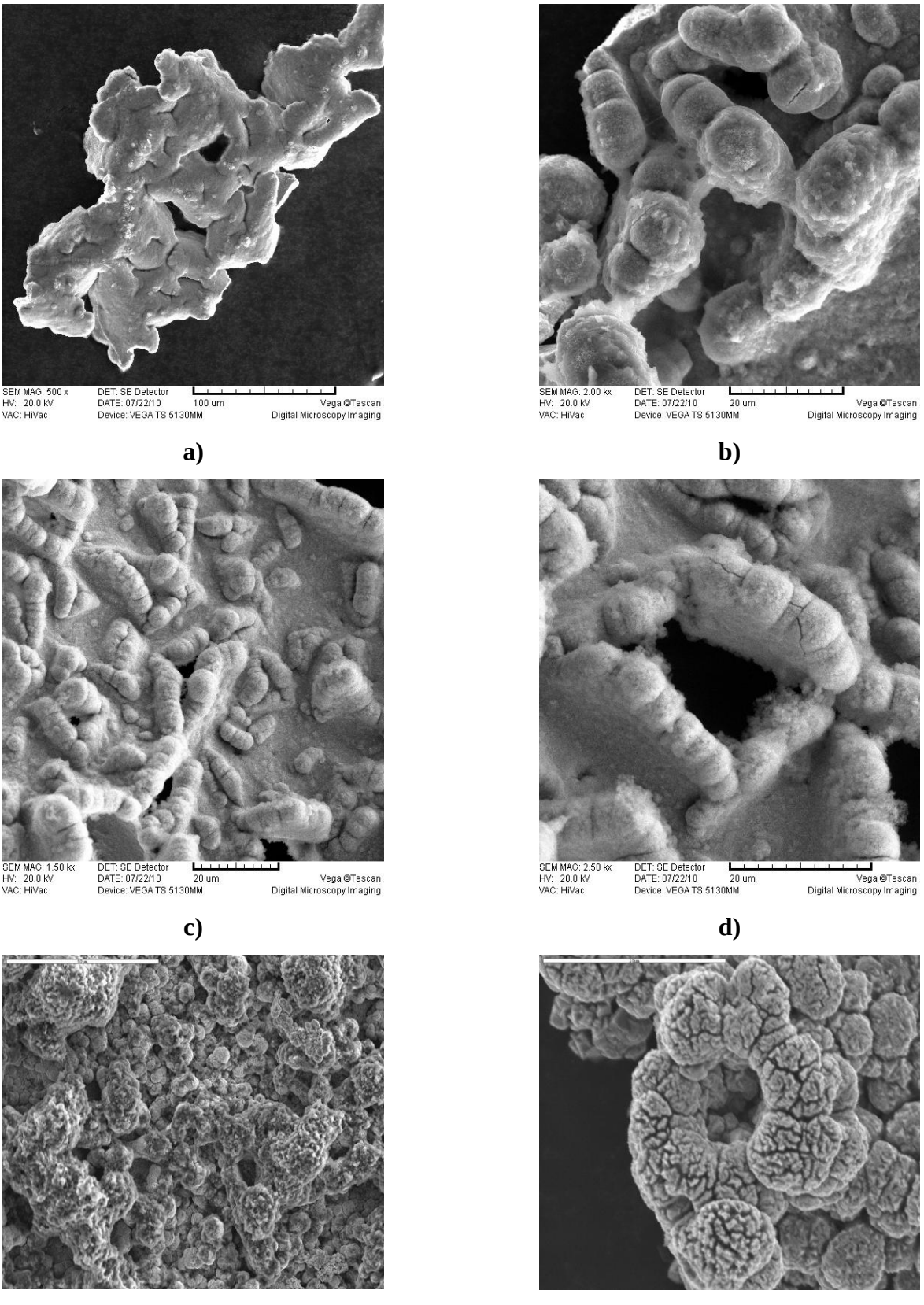

Figure 4. SEM micrographs of Fe powder onto glassy carbon electrode from the solution containing 0.1M Fe_2SO_4 x $7H_2O$ + 0.2M $Na_3C_6H_5O_7$ + 1.0M $(NH_4)_2SO_4$. Morphology of the powder particles (a, c, e); morphology of the surface (b, d, f). j = 0.4 Acm^{-2} (a, b); j = 0.5 Acm^{-2} (c,d) and j = 0.6 Acm^{-2} (e,f).

This is a consequence of intensive hydrogen evolution and its bubble formation (actually the process is defined by the rate of bubble formation), so that Fe deposit grows around the hydrogen bubble with the rate comparable to the rate of bubble growth. At the moment of powder particle detachment from the electrode surface bubble liberates itself and the cavity becomes characteristics of the powder particle. It should be noted that those two types of powder particles are almost equally distributed in the Fe powder for this case. At higher magnification, as shown in Figs. 4b, d and f, a cauliflower nature of the top surface of both types of powder particles is clearly visible (fragile film - in the form of agglomerates). In this case of electrodeposition of Fe powder particles a bigger size of about 250-400 μm are detected.

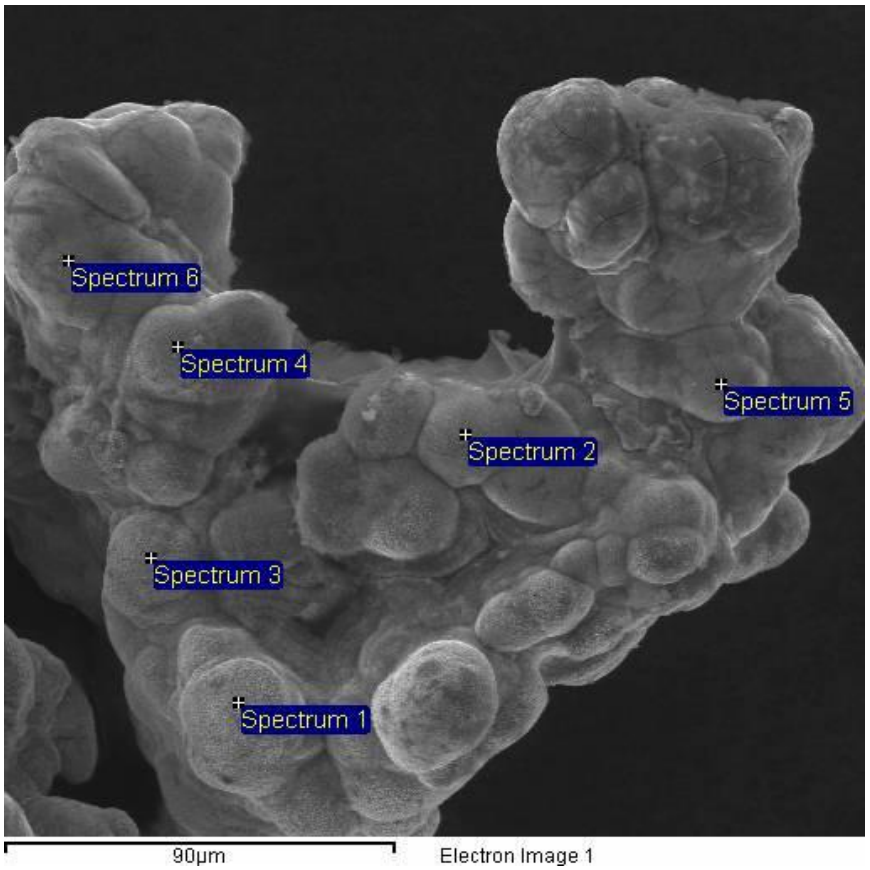

Spectrum	In stats.	O	Fe
Spectrum 1	Yes	5.39	94.61
Spectrum 2	Yes	4.36	95.64
Spectrum 3	Yes	6.39	93.61
Spectrum 4	Yes	3.95	96.05
Spectrum 5	Yes	5.37	94.63
Spectrum 6	Yes	6.36	93.64
Mean		5.30	94.70
Std. deviation		1.00	1.00
Max.		6.39	96.05
Min.		3.95	93.61

Figure 5. EDS analysis of Fe powder electrodeposited from the solution containing 0.1M Fe_2SO_4 x $7H_2O$ + 0.2M $Na_3C_6H_5O_7$ + 1.0M $(NH_4)_2SO_4$; j=0.6 A/cm^2. Mean content of Fe 94.70 at.%

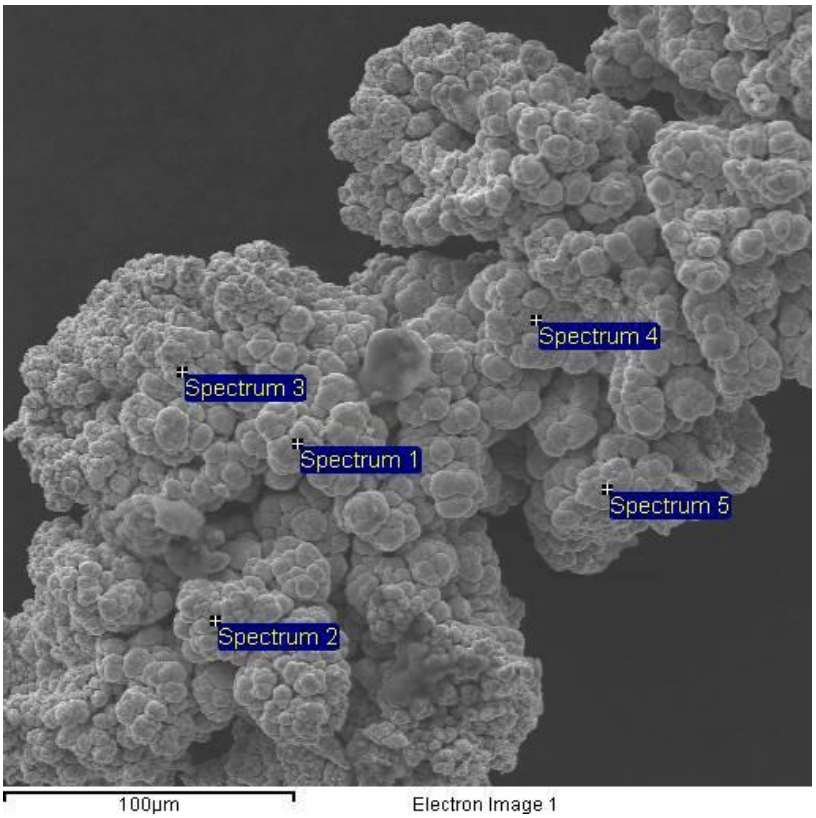

Spectrum	In stats.	O	Fe
Spectrum 1	Yes	14.17	85.83
Spectrum 2	Yes	6.46	93.54
Spectrum 3	Yes	7.13	92.87
Spectrum 4	Yes	3.72	96.28
Spectrum 5	Yes	8.45	91.55
Mean		7.99	92.01
Std. deviation		3.87	3.87
Max.		14.17	96.28
Min.		3.72	85.8

Figure 6. EDS analysis of Fe powder electrodeposited from the solution containing 0.1M $FeCl_2x4H_2O$ + 0.2M $Na_3C_6H_5O_7$ + 2.0M NH_4Cl; j=1.0 A/cm^2. Mean content of Fe 92.01 at.%.

Powders have a high chemical activity because of the large surface area and so, readily react with oxygen in air to form surface oxides [4,14,20]. It is known that corrosion processes occur at the boundary surface of a powder particles and the liquid phase. In this way, it is possible to imagine that moisture adsorption can be prevented by the formation of a film on the surface of the powder particles, which could enable their long-term and safe protection. In relation to this, it was necessary to find stabilizers that would enable the creation of hydrophobic adsorption films on the surface of the powder particles, which would be able to protect and stabilize the metal surface from the effect of moisture [20]. The assumption is that they stabilize by forming colloidal precipitates in the form of a protective film on the surface of particles.

Contents of the Fe and oxygen obtained by EDS analysis show that Fe deposited from citrate-chloride and citrate-sulfate supporting electrolytes is very good stabilized by sodium soap. Even more, a

soap solution treatment applied as a method of washing and drying provides good protection of Fe powders from oxidation (Figs. 5 and 6).

4. CONCLUSIONS

The main results obtained in this study can be summarized as follows: (1): Polarization diagrams recorded during the electrochemical deposition of Fe powders are characterized by the presence of two inflexion points, i.e. the first inflection corresponds to the beginning of metal deposition which is then followed by the rapid rise of current density, whereas the second inflection characterizes the start of a linear change of current density with potential. (2): The morphology and composition of obtained powders depend on the anion presence in the electrolyte. (3): A characteristic feature of powders deposited from citrate-chloride supporting electrolyte is cauliflower-like compressed structure. On the other side, Fe powders electrodeposited from citrate-sulfate supporting electrolyte appeared in the form of spongy and sticky agglomerates. Possibility of Fe powders protection from corrosion in the process of production and during long-term storing has been shown.

ACKNOWLEDGEMENT
This work was financially supported by Ministry of Science of the Republic of Serbia under the research project "Deposition of ultrafine powders of metals and alloys and nanostructured surfaces by electrochemical techniques" (142032G/2006).

References

1. R.Piontelli, *Proc. 2nd Meeting of CITCE,* (1950), Milan, Italy (1951) p. 163
2. S.Tajima and M.Ogata, *Electrochim. Acta,* 13 (1968) 1845
3. N.D.Nikolić, Lj.J.Pavlović, M.G.Pavlović and K.I.Popov, *J. Serb. Chem. Soc*., 72 (2007) 1369
4. V.D.Jović, B.M.Jović, V.Maksimović and M.G.Pavlović, *Electrochim. Acta*, 52 (2007) 4254
5. V.D.Jović, B.M.Jović and M.G.Pavlović, *Electrochim. Acta*, 51 (2006) 5468
6. A.Calusaru, *Electrodeposition of Powders from Solutions*, Elsevier, New York, NY, 1979, p.363
7. N.Kudryavtsevand V.Petrovna, *Novosti tehniki*, N.K.T.R., 171 (1932)
8. L.Kuzmin and V.Kiseleva, *Zhur. Prikl. Khim.,* 22 (1949) 311
9. C.Hardy and C.Mantell, F.P., No.814500 (1937)
10. C.Hardy and C.Mantell, USA Patent, No.2157699 (1938)
11. N.Kurdyavtsev and E.Tereshkovitch, *Zhur. Prikl. Khim.,* 12 (1948) 1298
12. M.Balshin, NIIMASH, 12 (1935) 5
13. H.Casey, USA.Patent, No.2481079 (1949)
14. V.M. Maksimović, Lj.J. Pavlović, B.M. Jović and M.G. Pavlović, *J.Serb.Chem.Soc.* 73 (2008) 861-870
15. B.M. Jović, V.D. Jović, V.M. Maksimović and M.G. Pavlović, „*Electrochim. Acta,* 53 (2008) 4796-4804
16. M.G. Pavlović, Lj.J. Pavlović, U.Č. Lačnjevac, N.D. Nikolić and M.V. Tomić, *Second Regional Symposiun on Electrochemistry-South-East Europe,* International Conference, Proceedings, SDE-P-21, pp. 201-205, ISBN 978-86-7132-044-3, 2010, Belgrade, Serbia
17. M.G. Pavlović, Lj.J. Pavlović, M.M. Pavlović and U.Č. Lačnjevac, *61st Annual Meeting of the International Society of Electrochemistry,* S08-ID-102153, CD of Abstracts, 2010, Nice, France.

18. Chin-Ming Chu, *J. Chin. Inst. Chem. Engrs.,* 34 (2003) 689
19. R.M. Khalil, *J. Appl. Electrochem.,* 18 (1987) 292
20. M.G. Pavlović, Lj.J. Pavlović, I.D. Doroslovački and N.D. Nikolić, *Hydrometallurgy*, 74 (2004) 155
21. H. Vogt and R.J. Balzer, *Electrochim. Acta* 50 (2005) 2073
22. H. Vogt, *Electrochim. Acta* 42 (1997) 2695
23. H. Vogt, *J. Appl. Electrochem.* 29 (1999) 137
24. R. Wüthrich, V. Fascio and H. Bleuler, *Electrochim. Acta* 49 (2004) 4005
25. R. Wüthrich and H. Bleuler, *Electrochim. Acta* 49 (2004) 1547
26. R. Wüthrich, Ch. Comninellis and H. Bleuler, *Electrochim. Acta* 50 (2005) 5242
27. N.D. Nikolić, K.I. Popov, Lj.J. Pavlović and M.G. Pavlović, *J.Electroanal.Chem.*, 588 (2006) 88
28. N. D. Nikolić, K.I. Popov, Lj. J. Pavlović and M.G. Pavlović, *Surface and Coatings Technology*, 201 (2006) 560
29. N.D. Nikolić, K.I. Popov, Lj.J. Pavlović and M.G. Pavlović, *Sensors*, 7 (2007) 1
30. N.D. Nikolić, Lj.J. Pavlović, M.G. Pavlović and K.I. Popov, *Electrochim. Acta*, 52 (2007) 8096
31. N.D. Nikolić, Lj.J. Pavlović, S.B. Krstić, M.G. Pavlović and K.I. Popov, *Chemical Engineering Science* 63 (2008) 2824
32. N.D. Nikolić, G. Branković, M.G. Pavlović and K.I.Popov, *J.Electroanal.Chem.* 621 (2008) 13
33. N.D. Nikolić, G. Branković, M.G. Pavlović and K.I.Popov, *Electrochemistry Communications*, 11 (2009)421
34. K.I. Popov, B.N. Grgur, M.G. Pavlović and V.Radmilović, *J. Serb. Chem Soc.* 58 (1993) 1055
35. Shin, H.-C., Dong, J., Liu, M., *Adv. Mater.* 15 (2003) 1610
36. Shin, H.-C., Liu, M., *Chem. Mater.* 16 (2004) 5460
37. Shin, H.-C., Liu, M., *Adv. Funct. Mater.* 15 (2005) 582
38. Yin, J., Jia, J., Zhu, L., *International Journal of Hydrogen Energy* 33 (2008) 7444
39. N.D. Nikolić, K.I. Popov, Lj.J. Pavlović and M.G. Pavlović, *J. Solid State Electrochem.* 11 (2007) 667